Ibn Al-Haitham Journal for Pure and Applied Sciences
Journal homepage: jih.uobaghdad.edu.iq
PISSN: 1609-4042, EISSN: 2521-3407
IHJPAS. 2024, 37(4)

Chitosan Reinforced Polyvinyl Alcohol and Nanoparticles Treatment to Promote Skin Wound Healing in Diabetes Induced Mouse Model

Huda R. Kttafah[1,*], Hanaa S. Mahmood[2] and Hussein N. Olewi[3]

[1]Department of Physics, Ministry of Education, Directorate General of Education Rusafa 2, Baghdad, Iraq.
[2]Department of Physics, College of Education for Pure Science, (Ibn Al-Haitham), University of Baghdad, Baghdad, Iraq.
[3]Department of Mechanical Engineering, College of Mechanical Engineering, University of Karabuk, Karabuk, Türkiye.
*Corresponding Author.

Received: 2 November 2023 Accepted: 8 January 2024 Published: 20 October 2024
doi.org/10.30536.37.4.3808

Abstract

A group of mice were captured. We divided the 3-month-old mice into groups. We limited each group to a specific type of treatment, using different components of silver (Ag) and gold (Au) in various proportions. The control group was left untreated. We stimulated her diabetes with injections of the substance alloxan, which led to the development of her condition. It was left for three days after the injection of this substance, and then the diabetes was checked with a diabetes testing device until all the required mice were infected with diabetes. Next, they removed the hair from the mouse's top and used a special tool, a ring with a diameter of 8 mm, to cut the skin. During the work, they used two types of anesthetics: ketamine and xylazine. The ketamine relaxes her muscles and causes her death, so she abandoned the xylazine and relied solely on the first type. The percentage of the anesthetic substance injected depends on its weight. Therefore, we created an incision on the mouse. Then I began treating the wounds: the first group with 100% AgNPs, the second group with 100% AuNPs, and the third group with samples of a mixture of AgNPs and AuNPs at a ratio of 50% each. The fourth and final group remained without treatment. With a weekly checkup for diabetes. The treatment entailed applying the sample to the wound and adhering it with a medical adhesive, periodically replacing it. After the second week of treatment, some of the wounds began to heal. By the end of the fourth week, it had completely healed. The group that was treated with the mixed samples had the best and fastest recovery and wound healing among the rest of the samples, followed by the mixture samples.

Keywords: Chitosan/PVA, nanoparticles, skin healing, diabetes.

1. Introduction

Skin physiological impairments in uncontrolled diabetes mellitus (DM) patients are frequently associated with delayed and challenging healing processes. In an animal-induced DM model, mimicking the wound phenotype would facilitate the assessment of wound-healing products and the healing duration period. We looked at how well chitosan/PVA-embedded Au and Ag nanoparticles helped wounds heal faster in a mouse model than alloxan-induced DM. We need modest and appropriate animal models in wound healing, and these trends are welcome in human

wound healing. Therefore, today's wound treatment is more effective and better understood than in the past. We aim to develop the most suitable animal model for human use, which also contributes to the healing and treatment of wounds.

Diabetes is chronic for many people who suffer from a deficiency in insulin secretion, which in turn leads to high blood sugar [1]. Diabetes is one of the most pressing global health issues in all countries. In the coming years, we expect the number of affected individuals to increase [2]. Diabetes is heat-resistant and affects all organs and tissues of the body, including the skin. A diabetic person faces the problem of faster wound healing compared to non-diabetic individuals [3]. Many diabetics suffer from skin problems, and this is obvious to them. They will easily develop skin diseases as they grow older [4]. It may lead to skin deformities associated with stress and pressure, poor growth factor production, poor blood vessel formation, and abnormal regulation of inflammatory products, all of which contribute to premature and accelerated skin aging [5]. It also contributes to the progression of skin infections. The inflammation may reach the deep layer of the skin and cause serious damage, which in turn is a medical burden [6].

Indeed, this is a significant warning sign for individuals with diabetes. The non-healing of the wound is attributed to a decrease in the production of fats in the skin, leading to dryness, and a decrease in the production of platelets, which are responsible for blood clotting in wounds [7]. It causes bleeding and increased inflammation. This may lead to the amputation of the affected part [8]. The environment in which the injured person lives plays a fundamental role in the patient's recovery, in addition to the new treatment. [9].

In this research paper, I investigated the effects of diabetes on the skin and how to treat wounds. The study found that diabetes accelerates the healing process in mice compared to non-infected mice [10]. Understanding the primary causes of skin complications in diabetic patients could aid in early diagnosis and treatment planning [11]. It has the potential to benefit humans and aid in their recovery from diabetes [12]. We utilized both natural and synthetic polymeric materials, including chitosan, chitosan, and polyvinyl alcohol. Chitosan was the basic material. We used prepared nanoparticles as solutions to boost the insulin levels of the diabetes-infected mice in this study, which consequently reduced their blood sugar levels [13].

2. Materials and Methods

We prepared the matrix, which is the chitosan powder, by mixing it with acetic acid and obtaining a homogeneous solution. Next, we prepared the reinforced material, powdered polyvinyl alcohol, by mixing it with distilled water. We then mixed the two solutions to create a single, homogeneous solution. Two types of nanoparticles, prepared in different proportions of both silver and gold, reinforced the resulting solution. Consequently, we acquired nanoscale samples to manage diabetic wound aggregates. Study design: experimental groups. The three treatments and the control group consisted of 4 BALB-c mice each (Tab the University of Baghdad College of Veterinary Medicine in Abu Ghraib, Iraq provided the BALB-c mice from their animal laboratory. We acclimatized the mice in special cages for two weeks, maintaining a temperature of 24 °C, medium humidity, and a light and dark cycle of 12–12 hours. ours. Access to drinking water and food was exceedingly easy [13].

Table 1. Experimental groups.

	Treatment groups			**Control**
Group #	**G1**	**G2**	**G3**	**G4**
# of mice	4	4	4	4
Treatment	100 % Ag NPs	100%AuNPs	(50%Ag+50%AuNPs)	no treatment

In BALB-c mice, alloxan-induced diabetes occurs. After a 12-hour fast, all four groups were given one or more intraperitoneal (IP) injections of alloxan (Serial No. AL1027B, 2-Alloxan (hydrate) 98%, Batch No. Aoo89B) by ALPHA CHEMIKA at a dose of 100 mg/kg of body weight, as explained in [14]. A diabetes-measuring device was used to collect a blood sample from the tail after three days of alloxan administration, we regularly tested the blood glucose single-point levels to confirm the induction of diabetes; the fasting glucometer readings were > 250 mg/dL. mg/dL. We dissolve the alloxan (100 mg powder) in 10 ml of distilled water and calculate the dosage as follows [15].

$$\text{Dosage in mg} = \frac{Body\ Weight\ of\ animal\ (g)}{1000\ g} * dose(mg) \quad (1)$$

We performed the wound generation on the back side of the mice's bodies in all four groups of animals **Figure 1** [16]. We sedated the animals with 0.1 mg/kg of BW ketamine (subcutaneous injection) and excised a skin circle-shaped punch (8 mm diameter) from the back of the mice. We applied the treatment using a wound dressing bandage, adhering it to the entire excision area and replacing it with a new one every week [17]. Every week, we take a skin biopsy to replace the dressing bandage treatment. We removed the initial skin, saved all subsequent biopsies in a buffer, and sent them for histopathological examination.[19].

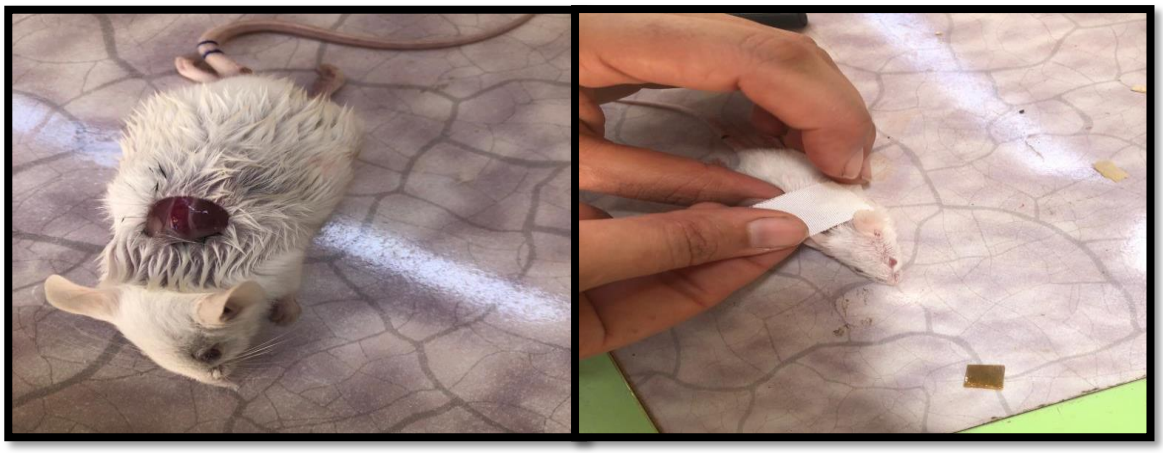

Figure 1. Skin wound generation and treatment application. Skin wound excision (circle shape 8mm in diameter) (left picture). Wound treatment using dressing bandages contains the Au, Ag NPs combination treatments as explained in the experimental group's Table 1. (right picture).

3. Results and Discussion

To characterize the tissues of the cells of the epidermis and dermis, we use the electron microscope, which is considered a complement to the histological analysis. Through the microscope, it is clear that the animal's skin structure is a difference in the structure of the skin of the animal. The organization of keratinocytes in mouse strains resembles a honeycomb. There were no microscopic pathological changes in the skin of the animals taken for both the negative control group and the animals of the other groups before treatment. As shown below in **Figure 2** [20], the epidermis and dermis compose the skin, characterized by their typical layers without the appearance of any lesions.

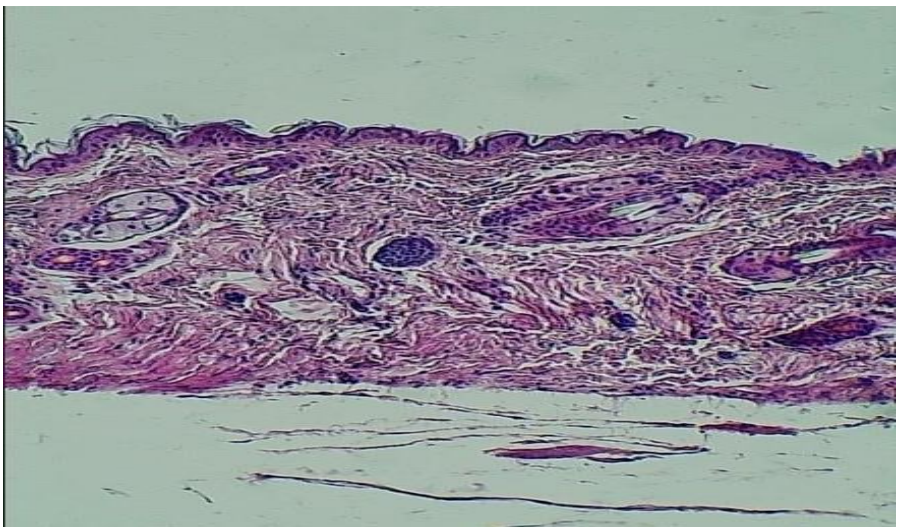

Figure 2. Histopathological figures for the section of skin for one animal in the control the negative group showed epidermis and dermis with no legion (H&E(X20)).

The control group, the positive group, showed thickening of the epidermis (layers) in all its layers, especially the stratum spinosum [21]. The cells showed necrosis (the presence of gaps) in the layers of the epidermis as well as proliferation of fibroblasts and generators, as shown in **Figure 3** [22].

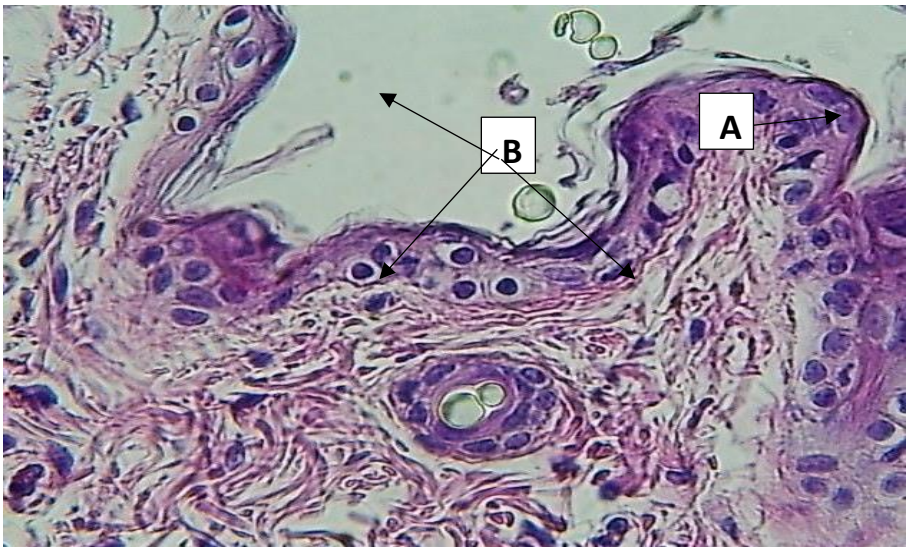

Figure 3. The histopathological figure for |section of skin for one animal in the control the Positive group showing thin new of epidermis vacuolation of call-in epidermis (A) proliferation of fibroblast (B) (H&E(X200)).

In addition to the infiltration of inflammatory cells in the epidermis and dermis layers and around the hair follicles, as shown in **Figure 4**[23].

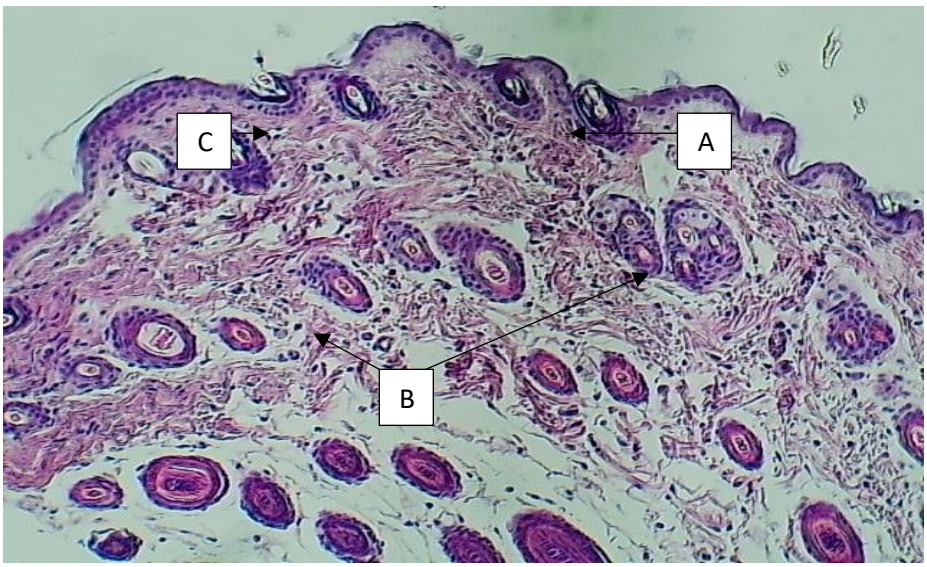

Figure 4. The histopathological figure for the section in skin for one animal in the control the Positive group induced by D.M shows thin new infiltration of the inflammatory cell (A) in addition to peri hair follicles accounting epidermis (B) and of number Phylis (C)(H&E(X200)).

Most of these cells are neutrophils[24]. It even collected neutrophil cells in some sections and also cleansed the abscess, as shown in **Figure 5**.

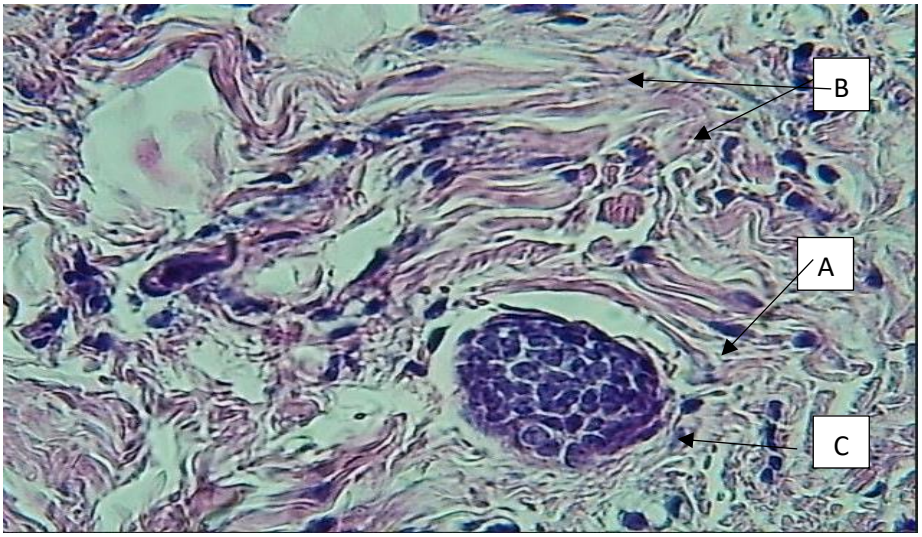

Figure 5. The histopathological figure for the section of skin for one animal in the control the Positive group showed abscessation of hair follicles (A) with the proliferation of fibroblast (B) and infiltration of inflammatory cells (C) (H&E(X400).

The histopathological changes in the group treated with silver nanoparticles showed fewer pathological changes than those found in the positive control group [25]. There were fewer thickenings than in the positive control, as shown in **Figure 6**. In addition to the presence of hyperplasia of hair follicles and fat cells, along with the proliferation of fibroblasts and fibroblasts[26].

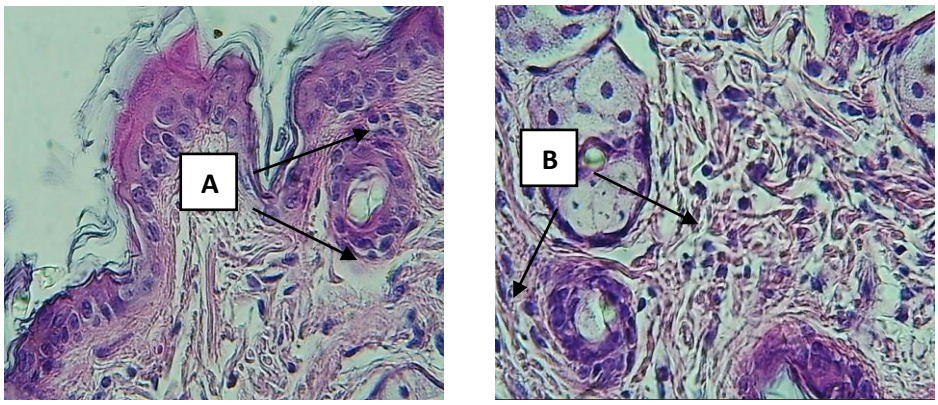

Figure 6. The histopathological figure for a section of skin for one animal in the 100% AgNPs treated group shows (A) Epidermis skin layer thickening and fibroblast proliferation. (B) hyperplasia of the hair follicles and the sebaceous glands. (H&E-stained skin lesion X40).

If you looked closely at the tissue changes in the group that was given gold nanoparticles, you could see that they had a net of fibrous connective tissues, inflammatory cells invading, and a lot of fibroblast cells and sebaceous glands rising [27]. Moreover, the positive pathological changes in the positive control group were more severe than those in the gold nanoparticle-treated group [28]. The severity of the inflammation in the gold group caused necrotic areas to appear in some sections, but they were minor [29].

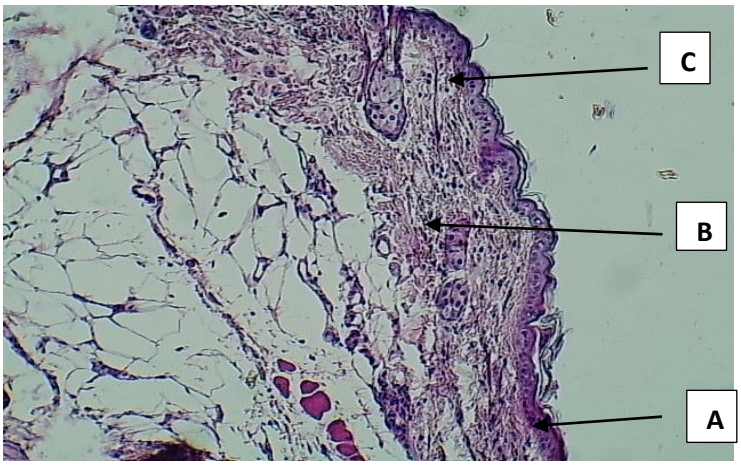

Figure 7. The histopathological figure for section Shows one animal treated with 100% AuNPs infiltration of the inflammatory cell(A) with fibrous connective tissues (B) and sebaceous glands (C)(H&E(X20)).

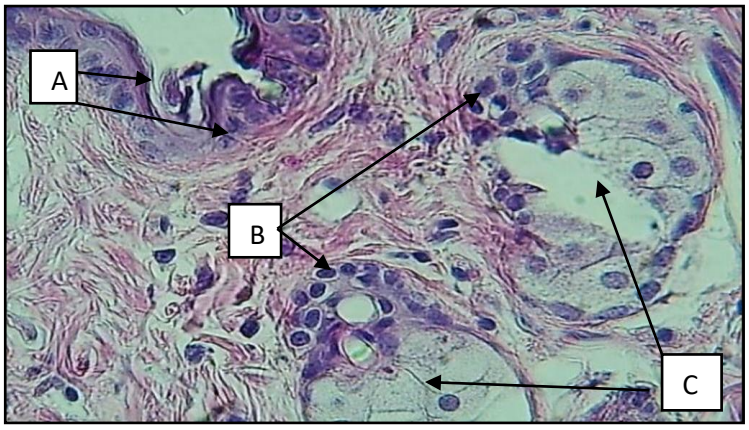

Figure 8. The histopathological figure for section Shows for one animal treated with 100% AuNPs Thickening of the epidermis (A), infiltration with inflammatory cells(B), and necrotizing of sebaceous glands (C) (H&E-stained skin lesion (X40)).

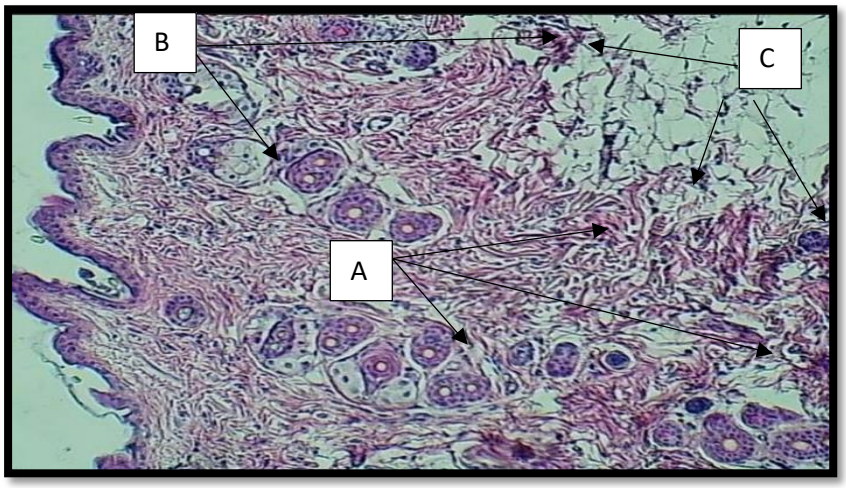

Figure 9. The histopathological figure for section Shows one animal treated with 100% AuNPs proliferation of the hair follicles (A), infiltration of inflammatory cells (B), and proliferation of fibroblast cells(C) (H&E-stained skin lesion (X200)).

The mixture group containing 50% AgNPs and 50% AuNPs exhibited very slight pathological changes. The treatment resulted in a noticeable and obvious improvement, as evidenced by the reduced thickening of the epidermis layer and the absence of inflammatory cell infiltration [30]. Noting that hair follicles and seborrheic cells were naturally present, even some sections were closer to normal (natural tissue), as shown in **Figure 10** and **Figure 11** [31]. concurring with Maycon Carvalho Ribeiro's research, which applied nanoparticles and chitosan to treat diabetic patients' wounds more quickly in rats. Also agreed with the researcher Paola Losi, who created an application to speed up wound healing in diabetes [32].

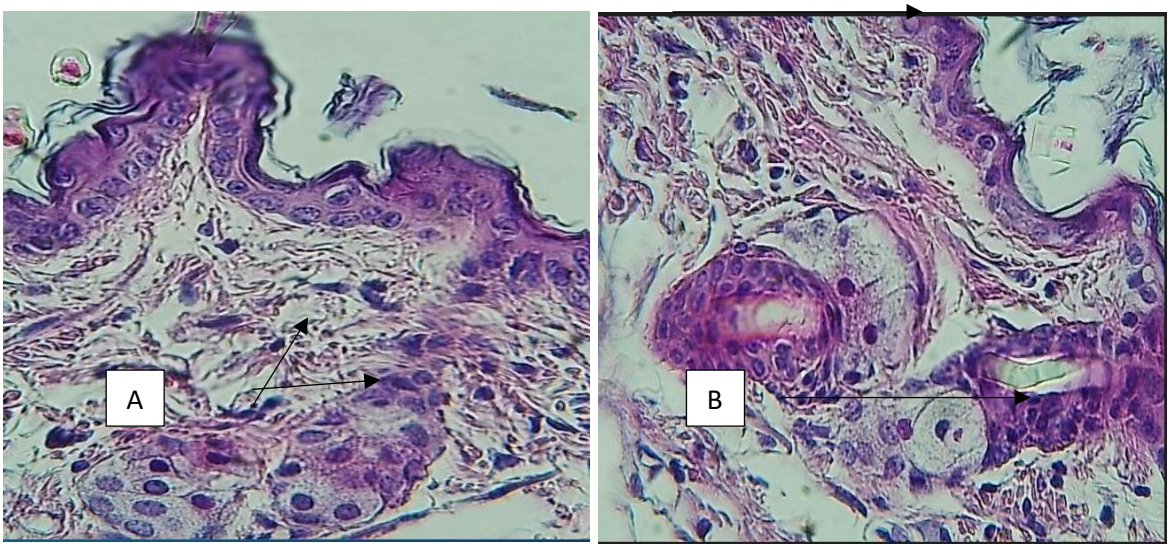

Figure 10. The histopathological figure for section Shows one animal treated with 50% AgNPs and 50% AuNPs mix treated group (A) with a slight thickening of the epidermis with few numbers of fibroblast (H&E-stained skin lesions (X10)). (B) normal hair follicles and the sebaceous glands (H&E-stained skin lesion (X40)).

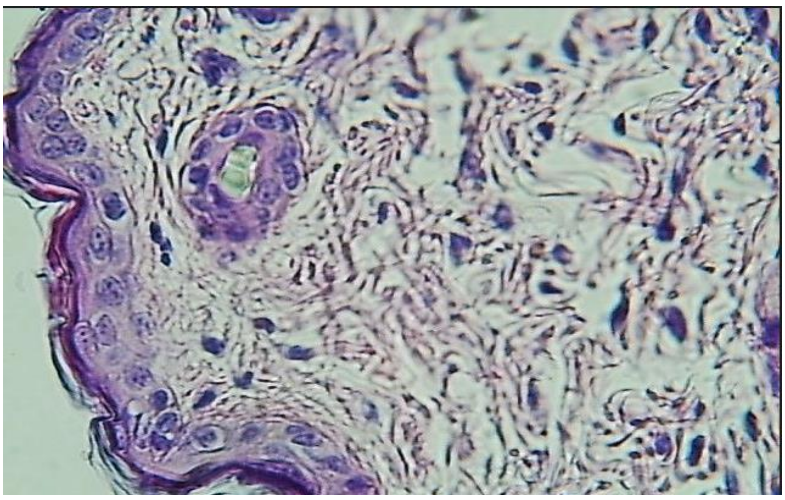

Figure 11. The histopathological figure for the section Shows that one animal treated with 50% AgNPs and 50% AuNPs mix treated group connective tissue is closer to natural (H&E-stained skin lesion (X40)).

This study found that there was a difference in response to treatment with nanoparticles among all groups. The group that received samples supported by a mixture of gold and silver nanoparticles in equal proportions achieved the best results. The group that received samples supported by gold nanoparticles came next. When the group was treated with silver nanoparticles, it responded less to treatment. The control group had skin infections, and recovery was very slow.

5. Conclusion

From the current study and through the use of nanoparticles in the treatment of diabetes, I found that using a mixture of silver and gold nanoparticles at a ratio of 50% of each has the greatest role in treating the wounds of diabetic patients, in addition to speeding up healing. This mixture is better than using each type of nanoparticle alone.

Acknowledgment

I would like to thank the staff of the Physics Department, Deanship of the College of Education for Pure Science (Ibn Al-Haitham) for their support in writing this research.

Conflict of Interest

The authors declare that they have no conflicts of interest.

Funding

None.

References

1. Sadiq K.; Mahmood, H.S. Enhancement of Antibacterial Activity of Face Mask with Gold Nanoparticles. *Ibn al-Haitham J Pure Appl Sci.* **2022,** *35(3),* 25-31. https://doi.org/10.30526/35. 3.2844
2. Karle, P.P.; Dhawale, S.C.; Mandade, R.J.; Navghare, V.V. Screening of Manilkara zapota (L) P. Royen stem bark ethanolic extract for in vitro α-glucosidase inhibition, preliminary antidiabetic effects, and improvement of diabetes and its complications in alloxan-induced diabetes in Wistar rats. *Bull. Natl. Res. Cent.* **2022,** *46(1),* 1–18. https://doi.org/10.1186/s42269-022-00783-3
3. Hofbauer, L.C. Bone fragility in diabetes: novel concepts and clinical implications. *Lancet Diabetes Endocrinol* **2022**, *23,* 45-65. https://doi.org/10.1016/S2213-8587(21)00347-8
4. Tice, M.J.; Bailey, S.; Sroga, G.E.; Gallagher, E.J.; Vashishth, D. Non-obese mkr mouse model of type 2 diabetes reveals skeletal alterations in mineralization and material properties. *JBMR plus.* **2022**, *6(2),* 10583, https://doi.org/10.1002/jbm4.10583
5. Khosla, S.; Samakkarnthai, P.; Monroe, D.G.; Farr, J.N. Update on the pathogenesis and treatment of

skeletal fragility in type 2 diabetes mellitus. *Nat. Rev. Endocrinol* **2021**, *17(11)*, 685–697. https://doi.org/10.1038/s41574-021-00555-5

6. Jbrael, Y.J.; Hamad, B.K. An Investigation into the Effects of Ubiquinone on Inflammation, Diabetic Myopathy and Endotheliopathy, and CBC Parameters in Diabetic Rats. *Ibn AL-Haitham J. Pure Appl. Sci.* **2023**, *36(2)*, 85–104. https://doi.org/10.30526/36.2.2976
7. Djabir, Y.Y. Artocarpus altilis leaf extract protects pancreatic islets and improves glycemic control in alloxan-induced diabetic rats. *J. Reports Pharm. Sci.* **2021,** *10(1)*, 87-99. https://DOI:10.4103/jrptps.JRPTPS5720
8. Kabach, I. Phytochemical profile and antioxidant capacity, α-amylase and α-glucosidase inhibitory activities of Oxalis pes-caprae extracts in alloxan-induced diabetic mice. *Biomed. Pharmacother* **2023**, *160*, 114393. https://doi.org/10.1016/j.biopha.2023.114393
9. Fadhil, I.N.; Al-Sarraf, A.R. Preparation and characterization of plastic wood from cellulosic residues. *Ibn AL-Haitham J. Pure Appl. Sci.* **2023**, *36(4)*,197–206. https://doi.org/10.30526/36.4.3230
10. Ahmed, E.; Alaubydi, M.A. A Comparative Correlation between the Oral Microbiome of Diabetes Mellitus and Healthy Individuals and their Relation with Some Demographic Parameters. *Ibn AL-Haitham J. Pure Appl. Sci.* **2023**, *36(4)*, 93–101. https://doi.org/10.30526/36.4.3133
11. Ayatollahi, S.A. Antidiabetic Activity of Date Seed Methanolic Extracts in Alloxan-Induced Diabetic Rats. *Pak. Vet. J.* **2019**, *39(4)*. 23-34. https://DOI:10.29261/pakvetj/2019.099
12. Arora, D.; Taylor, E.A.; King, K.B.; Donnelly, E. Increased tissue modulus and hardness in the TallyHO mouse model of early-onset type 2 diabetes mellitus. *PLOS One* **2023**, *18(7)*, 287825. https://doi.org/10.1371/journal.pone.0287825.
13. Onyibe, P.N.; Edo, G.I.; Nwosu, L.C.; Ozgor, E. Effects of Vernonia amygdalina fractionate on glutathione reductase and glutathione-S-transferase on alloxan-induced diabetes Wistar rat. *Biocatal. Agric. Biotechnol* **2021**, *36*, 102118. https://doi.org/10.1016/j.bcab.2021.102118
14. Al-Saadi, T.M. Investigating the Structural and Magnetic Properties of Nickel Oxide Nanoparticles Prepared by Precipitation Method. *Ibn Al-Haitham J. Pure Appl. Sci.* **2022,** *35(4)*, 94–103. https://doi.org/10.30526/35.4.2872
15. Ribeiro, M.C. Wound healing treatment using insulin within polymeric nanoparticles in the diabetes animal model. *Eur. J. Pharm. Sci.* **2020,** *150*, 105330. https://doi.org/10.1016/j.ejps.2020.105330.
16. Mahmood, H.S.; Jawad, M.K. Investigation of Chitosan/PEO Reinforced with AgNPs for Antibacterial Activity Prepared by Solution Casting Method. *Ann. Trop. Med. Public Heal* **2019**, *22(9)*, 70–82. https://doi.org/10.36295/ASRO.2019.220910
17. Eckhardt, B.A. Accelerated osteocyte senescence and skeletal fragility in mice with type 2 diabetes," *JCI insight* **2020**, *5(9)*. 34-45. https://doi:10.1172/jci.insight.135236
18. Ju, S.; Zhang, F.; Duan, J.; Jiang, J. Characterization of bacterial cellulose composite films incorporated with bulk chitosan and chitosan nanoparticles: A comparative study. *Carbohydr. Polym* **2020**, *237*, 116167. https://doi.org/10.1016/j.carbpol.2020.116167.
19. Fadhel, A.Q.; Jassim, W.H. Fabrication of Natural Gelcoats (Epoxy/Pumpkin Peels Fibers) Composites with High Mechanical and Thermal Properties. *Ibn AL-Haitham J. Pure Appl. Sci.* **2022**, *35(4)*, 21–36. https://doi.org/10.30526/35.4.2876
20. Garcia, C.E.G.; Martínez, F.A.S.; Bossard, F.; Rinaudo, M. Biomaterials based on electro spun chitosan. Relation between processing con DOI conditions and mechanical properties *Polymers* **2018,** *10(3)*, 23-34. https://doi:10.3390/polym10030257
21. Mahmood, H.S.; Habubi, N.F. Preparation of samarium doped- PMMA composite by casting method to evaluate the optical properties and potential applications. *J. Optoelectron. Adv. Mater.* **2023**, *25(2)*, 56–61.
22. Gao, Y.; Wu, Y. Recent advances of chitosan-based nanoparticles for biomedical and biotechnological applications. *Int. J. Biol. Macromol* **2022,** *203*, 379–388. https://doi.org/10.1016/j.ijbiomac.2022.01.162.

23. Labre, J.E.; Sroga, G.E.; Tice, M.J.L.; Vashishth, D. Induction and rescue of skeletal fragility in a high-fat diet mouse model of type 2 diabetes: An in vivo and in vitro approach. *Bone*. **2022**, *156*, 116302. https://doi.org/10.1016/j.bone.2021.116302.
24. Khesro, F.S.; Mahmood, H.S. Enhancement of Antibacterial Efficiency of Face Masks Using Metal Nanoparticles. *J. Pharm. Negative. Results* **2022,** *13(3)*, 178–182. https://doi:10.47750/pnr.2022.13.03.028
25. Mahmood, H.S.; Habubi, N.F. Structural, mechanical and magnetic properties of PVA-PVP: iron oxide nanocomposite. *Appl. Phys. A.* **2022,** *128(11)*, 956. https://doi.org/10.1007/s00339-022-06107
26. Mahmood, H.S.; Jawad, M.K. Antibacterial activity of chitosan/PAN blend prepared at different ratios. *in AIP Conference Proceedings, AIP Publishing LLC.* **2019**, *34*, 20078. https://doi.org/10.1063/1.5138564
27. Kttafah, H.R.; Khadim, A.I. The effect of dates palm trunk particles as improvement reinforcement material of polymeric composites and sustainable environmental material. *in AIP Conference Proceedings, AIP Publishing LLC.* **2019**, *12*, 20095. https://doi.org/10.1063/1.5117022
28. Farid, E.; Kamoun, E.A.; Taha, T.H.; El-Dissouky, A.; Khalil, T.E. PVA/CMC/Attapulgite Clay Composite Hydrogel Membranes for Biomedical Applications: Factors Affecting Hydrogel Membranes Crosslinking and Bio-evaluation Tests. *J. Polym. Environ* **2022**, *30(11)*, 4675–4689. https://doi.org/10.1007/s10924-022-02538-7
29. Paladini, F.; Pollini, M. Antimicrobial silver nanoparticles for wound healing application: Progress and future trends. *Materials (Basel)* **2019,** *12(16)*, 45-56. https://doi.org/10.3390/ma12162540.
30. Shao, X. Amelioration of bone fragility by pulsed electromagnetic fields in type 2 diabetic KK-Ay mice involving Wnt/β-catenin signaling. *Am. J. Physiol. Metab.* **2021,** *320(5)*, E951–E966. https://doi.org/10.1152/ajpendo.00655.2020.
31. Shehab, A.A.; Fadaam, S.A.; Abd, A.N.; Mustafa, M.H. Antibacterial Activity Of ternary semiconductor compounds $AgInSe_2$ Nanoparticles Synthesized by Simple Chemical Method. *in Journal of Physics: Conference Series, IOP Publishing.* **2018**, *345*, 12121. https://DOI:10.1088/1742-6596/1003/1/012121
32. Hassan, H.K. Study the physical and optoelectronic properties of silver gallium indium selenide AgGaInSe2/Si heterojunction solar cell. *in AIP Conference Proceedings, AIP Publishing* **2018**, *34*, 56-67. https://doi.org/10.1063/1.5039176